Analyst

Accepted Manuscript

ROYAL SOCIETY OF CHEMISTRY

www.rsc.org/analyst

Spirally-patterned pinhole arrays for long-term fluorescence cell imaging

Bon Ung Koo[1], YooNa Kang[2], SangJun Moon[2]*, and Won Gu Lee[1]*

[1]Department of Mechanical Engineering, College of Engineering, Kyung Hee University, 1732 Deokyoungdaero, Giheung, Yongin 446-701, Republic of Korea

[2]Cybernetics Laboratory, Robotics Engineering, DGIST, Republic of Korea

Abstract: Fluorescence cell imaging using a fluorescence microscope is an extensively used technique to examine the cell nucleus, internal structures, and others cellular molecules with fluorescence response time and intensity. However, it is difficult to perform high resolution cell imaging for a long period of time with this technique due to necrosis and apoptosis depending on the type and subcellular location of the damage caused by phototoxic damage. A large number of studies have been performed to resolve this problem, but they have struggled to meet the challenge between cellular viability and image resolution. In this study, we employ specially designed disc to reduce cell damage by controlling total fluorescent exposure time without deterioration of image resolution. This approach has many advantages in that the apparatus is simple, cost-effective, and easily integrated into the optical pathway through a conventional fluorescent microscope.

* These authors equally contributed to this work as corresponding authors.

PACS numbers: 07.60.Pb, 87.50.Hj

Keywords: fluorescence cell imaging; cell viability; pinhole disc

Corresponding authors

Drs. SJ Moon (nanobiomems@dgist.ac.kr) and WG Lee (termylee@khu.ac.kr)

Fax: +82-31-202-8106; Tel: +82-31-201-3321

1. INTRODUCTION

Fluorescence microscopy, along with the advances in nano/micro resolution imaging technologies, has been widely used in the field of biotechnology to observe internal structures and cellular processes for more than a decade. Fluorescent molecules respond to photons and move to a higher energy state. When fluorescence dye is injected into cells for dye infiltration inside the cytoplasm, fluorophores return to the ground state by emitting the energy as photons, enabling fluorescence imaging for a specific spatial resolution for the whole cell specimen, including its internal structures [1, 2]. This methodology allows identification of the distribution of specific markers inside cells and the ability to distinguish different kinds of cells through fluorescent tagging processes [3-5]. Moreover, the methodology is extensively used in fundamental studies on tumor cells for the diagnosis and treatment of cancers [6], in particular using nanoparticles as fluorescent dye, and has recently contributed in reducing operating time and enhancing accuracy in clinical practice [7]. However, fluorescence imaging causes phototoxic damage to cells during long-term exposure to the light source due to the direct injection of the fluorescent dye into the cell. When fluorescent substances infiltrate into cells, an abnormality in osmoregulation occurs primarily in the cell nucleus and internal structures. As a result, vesicles develop inside cells. Those vesicles affect the entire cell and eventually lead to necrosis as cell membranes rupture [8]. Phototoxicity can also lead to apoptosis, depending on the type and subcellular location of the damage [9, 10]. There are a number of methods that have been applied to resolve these problems. One practical method uses the effect of oblique-incidence reflection to regulate the intensity of the light source and also reduce exposure time to the light source [11]. Another study used controlled light exposure microscopy (CLEM) using software for fluorescence microscopy, and minimized overall cell injury by performing

fluorescence imaging only on target cells to reduce unnecessary cell damage in the periphery [12]. Although those methods effectively reduced cell damage caused by fluorescence effects, low resolution fluorescence images still remain as a problem to overcome. Currently, fluorescence imaging technology continues to seek techniques to improve image resolution while minimizing cellular damage caused by the low intensity light source required for fluorescent activation [13]. In recent years, researchers have developed some methods like near infrared fluorescent dyes which could minimize the effect of light on cells, which the nanoparticles show negligible toxicity [14]. As another approach of cell viability enhancement is introduced by filtering out the background of autofluorescence of cells and tissues, researchers have developed a technology combined with a long life time transition metal complex and by applying the time gating technique for the higher resolution of the cell imaging [15, 16].

To resolve these problems, a novel disc was developed by integrating a pinhole pattern on the Nipkow disc used in confocal microscopes. The pinhole disc is derived from the principle of the thaumatrope invented in the early 1800's, which relies on the principle to create optical illusions of motion using two pictures drawn on the two sides of a piece of cardboard which become one as the disc is rotated. The German scientist Paul Nipkow invented a scanning device called a Nipkow in 1884, and contributed to creating the first television pictures. In this apparatus, pinholes were arranged in a spiral pattern on a disc to project an image behind the disc through the pinhole array. The image projected through the pinhole disc is moved quickly, resulting in the illusion of a set of pictures as moving image. The pinhole disc is designed to allow imaging of objects with a relatively small number of photons [17].

When the pinhole disc rotates in the light path of a fluorescence microscope, the excitation light passes through a pinhole with constant fluorescence intensity. We devised a technique to

reduce the impact of fluorescence radiation on cells by blocking the excitation light repetitively at high speed while the disc part rotates without pinholes. In this paper, we aimed to obtain fluorescence imaging while reducing cell phototoxic damage during fluorescence exposure without deterioration of image resolution. Moreover, the suggested apparatus can be adapted to ordinary wide field of view microscopes, in addition to confocal microscopes without structural changes or complex manipulation of the hard/software instrument. Finally, we demonstrated appropriate improvement directions in performing high-quality fluorescence cell experiments by comparing the viability of fluorescence cells and the quantitative results of imaging resolution.

II. EXPERIMENTAL

1. Design of the patterned pinhole disc

The pinholes are arranged in a spiral pattern in a pinhole disc to observe the whole specimen evenly by making the angular velocities of inner and outer pinholes the same.

As shown in **Fig. 1a**, the spiral radius r_{ij} for jth pinhole of ith spiral (P_{ij}) is as follows:

$$\mathrm{r}_{ij}(\theta_{ij}) = \mathrm{f}(\theta_{ij}) = r_{i1} + \frac{iS_p}{2\pi}\theta_{ij}\ ,(\ i = 1, \dots, n\ and\ j = 1, \dots, m\ ) \quad (1)$$

where, r_{i1} is the innermost radius for the first pinhole (j = 1) of ith spiral, θ_{ij} is the angle between jth pinhole of ith spiral (P_{ij}) and the first start pinhole of ith spiral (P_{i1}), n is the number of spirals, m is the number of the pinholes in a spiral, and $S_p$is the pitch of the spirals. When the pinhole disc makes one revolution, the distance between start and end points is $n{\times}S_p$ and the radius becomes larger. Using r drawn with above variables, the spiral length of arc L is as follows:

$$L_{ij} = \int_0^{\theta_{ij}} f(\theta_{ij})\, d\theta = r_{i1}\theta_{ij} + \frac{iS_p}{2 \cdot 2\pi}{\theta_{ij}}^2 \quad (2)$$

When Eq. (2) is represented in terms of θ_{ij},

$$\theta_{ij} = \left(\frac{2\pi}{iS_p}\right)\left[-r_{i1} + \left(r_{i1}^2 + \frac{iS_pL_{ij}}{\pi}\right)^{\frac{1}{2}}\right] \quad (3)$$

The following Equations (4) - (6) are obtained from Equations (1) and (3).

$$L_{ij} = P_Lj = S_Pj\ (\text{where, put}\ P_L = S_p) \quad (4)$$

$$\theta_{ij} = \left(\frac{2\pi}{iS_p}\right)\left[-r_{i1} + \left(r_{i1}^2 + \frac{S_p^2 ij}{\pi}\right)^{\frac{1}{2}}\right] \quad (5)$$

$$r_{ij} = r_{i1} + \frac{iS_p}{2\pi}\theta_{ij}$$

$$= r_{i1} + \frac{iS_p}{2\pi}\left(\frac{2\pi}{iS_p}\right)\left[-r_{i1} + \left(r_{i1}^2 + \frac{S_p^2 ij}{\pi}\right)^{\frac{1}{2}}\right]$$

$$= r_{i1} + S_p\left(\frac{ij}{\pi}\right)^{\frac{1}{2}} \quad (6)$$

We put the pitch of spirals into the same distance between pinholes as shown in **Fig. 1b**. Pinholes arranged in a spiral pattern could be obtained using equations (5) and (6) [18]. Following the design rules and the equations, an example pattern of the AutoCAD™ design of the pinhole discs is shown in **Fig. 1c**, which follows the parameters to design the number of spirals at six and a 114 pinhole array for each spiral.

2. Development of a pinhole disc module

Using the equations for the pinhole pattern in Section 2.1, the pattern of the pinhole disc was designed using AutoCAD™, which gives the position of the pinholes and the angle between pinholes. To make n × S_p fit into an inner circular diameter of 8mm, the outmost circular diameter was set as 10 mm with tolerance of ±1, and the study established spiral numbers as 6, the diameter of the pinhole as 0.5 mm, and the distance between pinholes to be 1.17 in disc

designing which is based on the penetration rate of fluorescence. **Table 1** represents the specification of a pinhole disc module, and shows interpreted data for exposure and non-exposure times to fluorescence per pinhole and the ratio of exposure: non-exposure according to the pinhole disc rotation speed, which was chosen by following a total normalized exposure time of one second. The ratio of exposure: non-exposure of the disc in the study was set into 1:2.34 following the design parameters of the pinhole arrays and spirals. When the pinhole disc rotates with a constant angular velocity, ω, cells were exposed to fluorescence light that had passed through pinholes for a second, while cells were not exposed to the radiation for 2.34 seconds due to physical interruption in light flow by the disc surface. The fluorescence light intensity was 100% when light passed through the pinholes intact. On the other hand, light intensity was 0% in the disc area without pinholes. Thus, cells exposed to the light while rotating the disc were being exposed to the fluorescence effects at an average intensity of about 30% compared to cells without disc pinholes. The exposure intensity could also be controlled by a pulse wide modulation (PWM) approach. The pinhole disc was fabricated by attaching the pattern to an easily purchasable small empty CD. The designed Nipkow disc was then installed at the DC motor, on which a switch and a stand were equipped to facilitate a constant angular velocity as shown in **Fig. 2**. These apparatus were designed for two separate tests, a UV exposure test and a cell imaging test using a modified pinhole disc module. The UV curable resin exposure test apparatus is set into a UV protective groove box with external a UV light source, which requires high intensity UV to cure the resin as shown in **Fig. 2a**. The other rotated pinhole disc module was designed for cultured cell imaging using a conventional fluorescent microscope, which can be easily integrated into a conventional microscope system and culture dish as shown in **Fig. 2b**.

The designed pinhole disk modules were examined to verify the effectiveness of fluorescent light blocking and flushing by rotation speed of the pinhole arrays. Modulation of the UV light exposure rate was examined in a UV curable resin prior to the cellular substrate exposure test by the altering the rotation rate of the pinhole disc module which changes the total energy of exposed UV light. Modulation of the UV light exposure rate was analyzed by measurement of resin hardening which was modulated by applying the pinhole disc module in the UV curing system. The UV curable resin experiment aimed to identify the degree of light impact on resins, since the intensity of radiation energy varies as UV radiation projected to the rotating pinhole disc perpendicularly passes through pinholes. In this way, the curing degree of resin is identifiable with the color change after cross-linking, and the exposure energy of the fluorescence microscope is conveniently presumable with respect to the suggested pinhole disk module. The exposure time was set at a 30 second duration since the UV curable resin was cross-linked completely in 30 seconds with UV exposure at 225 mW/cm^2 average intensity in the condition of direct exposure. When the pinhole disc module was exposed to UV radiation for more than 90 seconds, the UV curable resin did not harden further because the time needed to reach the minimum energy to cross-link the polymer network is less than 90 seconds in the given exposure conditions. Based on the maximum exposure duration, 90 seconds, the experiments in the UV curing system with the pinhole disc module were performed at 30 second intervals, up to 90 seconds.

The results of the resin experiment in the UV curing system using the pinhole disc module are shown in **Fig. 3**. The irradiation rate in percentage with respect to the pinhole opening ratio was controlled by the designed spiral pattern, which can be determined from the motor rotation speed. The designed exposure rate was 1:2.3 for one revolution and average intensity of fluorescence

with respect to opening time was 32% for the fabricated pinhole disc module when one disc rotation time was set on 523.6 rad/sec as shown in **Fig. 3a**. Based on the designed hardware setup and exposure conditions, UV curable resin was analyzed for different exposure time durations. The hardening rate of the UV curable resin with and without using the pinhole disc module was measured according to exposure times up to 90 seconds with three different samples. At 90 seconds of exposure without the pinhole disc module, resin cured completely as usual with a 100% hardening rate of resin. However, by using the pinhole disc module, resins cured incompletely after exposure at 30 seconds, 60 seconds, and 90 seconds as shown in **Fig. 3b**. At 30 seconds of exposure, the hardening rate of resin progressed only about 30% compared to the standard curing condition, i.e. 90 seconds exposure without the pinhole disc module. When a 32% exposure duration is fixed with the pinhole geometry, the hardening rate of resin shows a linear relationship with the exposure time in the second time unit. This results shows whether lowering the intensity of excitation will have the similar effect since overall exposure time only affect the hardening rate of resin comparing to the total energy of the excitation light as shown in Fig 3b.These results also suggest that the fluorescence effects at average intensity can be designed according to the designed hardware disc specifications and rotation conditions.

3. Cell exposure experiment in a fluorescence environment

The cell exposure experiment in a fluorescence environment demonstrated that the pinhole disc module effectively reduced cell damage through light reflection and a relaxation time for specimens. The effects of fluorescence on cells were measured by installing the pinhole disc module into a conventional fluorescence microscope. Healthy HeLa cells were used as specimen

cells with a 95% confluence and over 96% viability after a normal culture condition. The light source for fluorescence was a 120W Xenon Burner and a 488 nm wavelength filter was equipped on both the conventional microscope and the pinhole disc module during the 90 second exposure experiment. The exposure time for fluorescence was set at 90 seconds to examine the state of cell viability before photobleaching, which occurs approximately 90 seconds after exposure to fluorescence. The time was also comparable with the UV curable resin experiment. For the control experiment, the viability of HeLa cells was measured without installing the pinhole disc module under the standard conditions used in the UV curable resin experiment with fluorescent and without fluorescent exposure. For the cell exposure experiment in the fluorescence environment, the pinhole disc module was installed in the light path of the conventional fluorescent microscope to compare the viability of HeLa cells with that of the control experiment. To verify the major factor of cell death during fluorescence exposure, we examined the apoptotic cell death rate of HeLa cells to differentiate between programmed cell death, apoptosis, and necrosis and depending on the type and subcellular location of the damage caused by external fluorescent damage. The viability of HeLa cells was measured by staining the cells with Trypan blue dye and was analyzed using the EVE^{TM} (NanoEnTek Inc., Korea) for image interpretation. The confluence of HeLa cells was calculated with the JuLi^{TM} BR (NanoEnTek Inc., Korea) and the apoptotic rate of HeLa cells was measured using the Tali^{TM} (Invitrogen^{TM}, USA).

III. RESULTS AND DISCUSSION

The viability of HeLa cells was measured by staining the cells with Trypan blue dye and was analyzed by using the EVE^{TM} (NanoEnTek Inc., Korea) for image interpretation as shown in **Fig. 4**. Comparison of cell viability was measured after the pinhole disk module exposure with cultured HeLa cells. The viability of HeLa cells decreases with no fluorescence, exposure to fluorescence for 90 seconds with the pinhole disc module, and the standard fluorescence imaging method without the pinhole disc module as shown in **Fig 4a**. The viability of HeLa cell was counted after Trypan blue-stained HeLa cells' live/dead images which was measured with the EVE instrument and software as shown in **Fig. 4b (i)** no exposure to fluorescence, **Fig. 4b (ii)** fluorescence exposure and with the pinhole disc module, and **Fig. 4 b (iii)** fluorescence exposure without the pinhole disc module, respectively. Without any fluorescent light stimulation to the cultured HeLa cells, healthy cells could be observed at a viability of up to 96% after cells grew to confluence. On the other hand, cell viability decreased markedly to about 20% when the specimen was exposed to fluorescence illumination for 90 seconds. When the pinhole disc module was installed in the conventional fluorescent microscopy along the light path, cell viability increased to about 75%. Although lower than that of cells without the influence of fluorescence, the 75% viability rate demonstrates the pinhole disc module effectiveness on live cells. And while the survival rate for the pinhole disc module, 70% in average value, is slightly lower than the control experiment, 96% in average value, the ratio of dead cells decreased remarkably compared to the no pinhole disc module case. The above results indicate that the use of the pinhole disc module reduced the effect of fluorescence on cells in fluorescence cell imaging tests.

There are two major factors for cell death. One factor is natural cell death during the culture process and the other is external light stimulation which effects cell viability during long-term culture. The apoptotic cell death rate of HeLa cells was examined to differentiate programmed cell death caused by external fluorescent damage. To verify the effect of natural cell death and the major factor of cell death during fluorescence exposure, we examined HeLa cells under three types of culture conditions for 72 hours as shown in **Fig. 5.** The figure shows a comparison of live, dead, and apoptotic cells with no fluorescence, exposure to fluorescence for 90 seconds with the pinhole disc module, and standard fluorescence imaging method without the pinhole disc module. Without any stimulation, **Fig. 5a** (black line) and **Fig. 5b (i)** (using Tali^{TM}), healthy cells could be observed at a death and apoptotic rate of below 5% with respect to the Live/Dead count. On the other hand, the death and apoptotic rate of cells indicate about 42% and 1% each when the specimen was exposed to fluorescence illumination for 90 seconds as shown in **Fig. 5b (ii)** and **(iii)**. This means most of the cells are damaged by the fluorescence, and do not die due to programmed cell death during long-term culture.

When a pinhole disc was installed in the light path, the death rate of cells was reduced to about 28% showing that the cell damage due to fluorescence was decreased. The fluorescence images of HeLa cells with and without the pinhole disc module and the schematic graph can be used to determine the optimal point of fluorescent imaging by adjusting disc rotation speed for viability and visibility compensation as shown in **Fig. 6**. The optimal exposure time can be determined by changing the disc rotation speed when the visibility increases as viability decreases. Based on both cell size distribution for the live (blue) and dead (red) cells in **Fig. 6a** and the fluorescence images of HeLa cells in **Fig. 6c** with the pinhole disc module for long and short-term exposure (90 and 30 seconds), one exposure example for the special application can be determined at 1μm

visibility with 75% viability at 90 seconds exposure time as shown in **Fig. 6b**. Without use of the pinhole disc module, fluorescence imaging provided clear, high-contrast cell images with a resolution up to 0.66 μm. In contrast, cell images with increased viability using the pinhole disc module showed a lower resolution of 2 μm.

IV. DISCUSSION

Controlling total fluorescent exposure time without deterioration of image resolution by the pinhole disc has many advantages in that the apparatus is simple, cost-effective, and easily integrated into the optical pathway through a conventional fluorescent microscope. Recently, the light-sheet fluorescence microscopy (LSFM) technology has emerged as an important imaging tool in live 3D samples over time with reduced phototoxicity and photobleaching [19]. LSFMs are adopted to mitigate the photodamage to live cell imaging. This approach also enables live 3D biological data for imaging of transparent tissues and whole organisms in developmental biology since it can reduce the photodamage during a long-term three-dimensional imaging process [20]. The LSFM utilizes a plane of light which is exposed toxic fluorescent light over imaging area not through an entire depth but a target depth [21]. Based on the method of thin light plane exposure, an optical sectioning, fluorophore bleaching, and phototoxicity of biological samples are minimized compared to wide-field fluorescence, confocal, and multiphoton microscopy. LSFMs produce serial sectioning images that are combined for three-dimensional reconstruction of tissue since at high spatiotemporal resolution. Light-sheet imaging is also widely adopted as a method for understanding neuronal circuit function based on the high resolution aspect [22].

Comparing to these advantages of the LSFM technology with the pinhole disc approach, the live 3D imaging using the pinhole disc could not be achieved because of low spatiotemporal resolution. However, numerous versions of light sheet microscopes is hard to be integrated with the conventional fluorescent microscopy because of a lack of a commercial LSFM microscope. Although problems still exist in observing fluorescent images through a microscope due to low resolution and photo-damage, the pinhole disc module can be integrated into the fluorescence microscopy which is anticipated to be widely used in experiments on cells or materials sensitive

to fluorescence imaging by reaching an optimal point between resolution and cell injury. The pinhole disc module can be one of a candidate for easy, cheap, and functional platform to reduce photo-damage of specimen comparing to the LSFM technology.

V. CONCLUSION

This study described the design and manufacture of a pinhole disc using a simple method. First, changes of resin composites in UV curing system and the survival rate of sample cells were assessed. Second, the study was able to observe cells using a fluorescence microscope by minimizing the existing disadvantage of cell injury caused by fluorescent dye. Although problems still exist in observing fluorescent images through a microscope due to low resolution, fluorescence microscopy is anticipated to be widely used in experiments on cells or materials sensitive to fluorescence imaging by reaching an optimal point between resolution and cell injury through advancements in insertion location and design of the pinhole disc module. Moreover, further studies on the photo bleaching phenomenon, in addition to cell viability, will enable investigators to perform long-term, high-quality fluorescence imaging experiments.

Acknowledgements This research was supported by the National Research Foundation of Korea (NRF-2012029193) and Basic Science Research Program through the NRF, funded by the Ministry of Science, ICT and Future Planning (2013010861). This study was also supported by a grant of the Korean Health Technology R&D Project, Ministry of Health & Welfare, Republic of Korea (HI14C1632). This work was supported by the IT R&D program of MSIP/KEIT (10041145, Self-Organized Software platform (SoSp)) for Welfare Devices and the DGIST R&D Program of the Ministry of Science, ICT & Future Planning (14-BD-06).

Author contributions WGL suggested the idea, designed the experiments, and analyzed the results. BUK fabricated the devices, conducted the experiments, and analyzed the images. WGL and BUK wrote the paper. KUN and SJM designed the experiments, and analyzed the results, and wrote the paper. WGL and SJM supervised all the process in each side as corresponding authors

REFERENCES

1. Stephens, D.J. and V.J. Allan, *Light microscopy techniques for live cell imaging.* Science, 2003. **300**(5616): p. 82-6.
2. Petty, H.R., *Fluorescence microscopy: established and emerging methods, experimental strategies, and applications in immunology.* Microsc Res Tech, 2007. **70**(8): p. 687-709.
3. Galdeen, S.A. and A.J. North, *Live cell fluorescence microscopy techniques.* Methods Mol Biol, 2011. **769**: p. 205-22.
4. Kim, K., et al., *Seeing the electroporative uptake of cell-membrane impermeable fluorescent molecules and nanoparticles.* Nanoscale, 2012. **4**(16): p. 5051-8.
5. Yun, K., et al., *Microscopic augmented-reality indicators for long-term live cell time-lapsed imaging.* Analyst, 2013. **138**(11): p. 3196-200.
6. Jeong, J., et al., *Color-tunable photoluminescent fullerene nanoparticles.* Adv Mater, 2012. **24**(15): p. 1999-2003.
7. Nguyen, Q.T., et al., *Surgery with molecular fluorescence imaging using activatable cell-penetrating peptides decreases residual cancer and improves survival.* Proc Natl Acad Sci U S A, 2010. **107**(9): p. 4317-22.
8. Kroemer, G., et al., *Classification of cell death: recommendations of the Nomenclature Committee on Cell Death.* Cell Death Differ, 2005. **12 Suppl 2**: p. 1463-7.
9. Oliveira, C.S., et al., *Major determinants of photoinduced cell death: Subcellular localization versus photosensitization efficiency.* Free Radical Biology and Medicine, 2011. **51**(4): p. 824-833.
10. Buytaert, E., M. Dewaele, and P. Agostinis, *Molecular effectors of multiple cell death pathways initiated by photodynamic therapy.* Biochimica Et Biophysica Acta-Reviews on Cancer, 2007. **1776**(1): p. 86-107.
11. Landry, S., et al., *Monitoring live cell viability: Comparative study of fluorescence, oblique incidence reflection and phase contrast microscopy imaging techniques.* Opt Express, 2004. **12**(23): p. 5754-9.
12. Hoebe, R.A., et al., *Controlled light-exposure microscopy reduces photobleaching and phototoxicity in fluorescence live-cell imaging.* Nat Biotechnol, 2007. **25**(2): p. 249-53.
13. Yamagata, K., et al., *Fluorescence cell imaging and manipulation using conventional halogen lamp microscopy.* PLoS One, 2012. **7**(2): p. e31638.

14. Yu, J., et al., *Near-infrared fluorescence imaging using organic dye nanoparticles.* Biomaterials, 2014. **35**(10): p. 3356-3364.
15. Huang, K.W., C.M. Jiang, and A.A. Marti, *Ascertaining Free Histidine from Mixtures with Histidine-Containing Proteins Using Time-Resolved Photoluminescence Spectroscopy.* Journal of Physical Chemistry A, 2014. **118**(45): p. 10353-10358.
16. Cook, N.P., et al., *Sensing Amyloid-beta Aggregation Using Luminescent Dipyridophenazine Ruthenium(II) Complexes.* Journal of the American Chemical Society, 2011. **133**(29): p. 11121-11123.
17. Walter, D., *History of television.* Adv Ophthalmol, 1976. **33**: p. 72-4.
18. Tanaami, T., et al., *High-speed 1-frame/ms scanning confocal microscope with a microlens and Nipkow disks.* Appl Opt, 2002. **41**(22): p. 4704-8.
19. Lim, J., et al., *Light sheet fluorescence microscopy (LSFM): past, present and future.* Analyst, 2014. **139**(19): p. 4758-4768.
20. Stelzer, E.H.K., *Light-sheet fluorescence microscopy for quantitative biology.* Nature Methods, 2015. **12**(1): p. 23-26.
21. Santi, P.A., *Light Sheet Fluorescence Microscopy: A Review.* Journal of Histochemistry & Cytochemistry, 2011. **59**(2): p. 129-138.
22. Keller, P.J., M.B. Ahrens, and J. Freeman, *Light-sheet imaging for systems neuroscience.* Nature Methods, 2015. **12**(1): p. 27-29.

Table 1. Design specifications for a pinhole disc module. Based on the number of pinholes and spirals, the total UV exposure time could be calculated using the disc rotation speed which is controlled by input voltage to maintain a constant angular velocity for an apparatus as shown in **Figure 2**.

Numerical Interpretation		
Angular velocity of pinhole disc	ω	523.6 rad/s
Linear velocity of pinhole	v	15.71 m/s
Diameter of pinhole	d_p	0.5 mm
Number of pinhole	m	114
Distance between pinholes	P_L	1.17 mm
Number of spirals	n	6
Distance (Pitch) between spirals	S_p	1.17 mm
Exposure time to fluorescence per pinhole	t_p	0.032 ms
Non-exposure time to fluorescence per distance between two pinholes	t_n	0.0745 ms
Ratio of exposure : non-exposure		1 : 2.34

Legend of Figures

Figure 1. Design parameters for pinhole arrays and number of spirals to observe the whole specimen evenly by making the angular velocities of inner and outer pinholes the same. (a) Related design parameters and nomenclatures for n number of spirals and m number of pinhole arrays, (b) enlarged figure for the notation of pinhole specification and its position with a pitch of spirals, S_p, distance between each pinholes, P_L, and pinhole diameter, d_p, (c) example pattern of the AutoCAD^{TM} design of pinhole discs, which follows the parameters to design the number of spirals at six and a 114 pinhole array for each spiral.

Figure 2. Schematic and photograph image of the UV exposure test and the cell imaging apparatus using a modified pinhole disc module. (a) UV curable resin exposure test apparatus using a rotated pinhole module which is set into a UV protective groove box, (b) cultured cell imaging apparatus using a conventional fluorescent microscope and a rotated pinhole disc module, which can be easily integrated into the conventional microscope system.

Figure 3. The results of the resin experiment in the UV curing system using the pinhole disc module. (a) Exposure rate (1:2.3) and average intensity of fluorescence (32%) onto a pinhole according to one disc rotation time with speed (523.6 rad/sec), (b) hardening rate of the UV curable resin with and without using the pinhole disc module according to exposure times up to 90 seconds. Three different samples were tested at each exposure time to measure the hardening rate of resin. When 32% exposure duration is fixed with the pinhole geometry, the hardening rate of resin shows a linear relationship with the exposure time in the second time unit.

Figure 4. Cell viability test after pinhole disk exposure with cultured HeLa cells. (a) Comparison of viability of cells with no fluorescence, exposure to fluorescence for 90 seconds with the pinhole disc module, and the standard fluorescence imaging method without the pinhole disc module, (b) Trypan blue-stained HeLa cells' live/dead images measured with the EVE instrument and software: (i) no exposure to fluorescence, (ii) fluorescence exposure with the pinhole disc module, (iii) fluorescence exposure without the pinhole disc module.

Figure 5. Confluence test after pinhole disk exposure with Live/Dead/Apoptotic cell death counting. (a) Time vs confluence of the cultured cells, (b) Confluence results of three types of HeLa cells cultured for 72 hours, (i) no exposure to fluorescence, (ii) fluorescence exposure with pinhole disc, (iii) fluorescence exposure without pinhole disc.

Figure 6. Schematic drawing for the optimal point of fluorescent imaging by adjusting disc rotation speed for viability and visibility compensation. (a) Optimal exposure time can be determined by changing the disc rotation speed. When the visibility increases, viability decreases. One example of the application can be to determine 1 um visibility with 75% viability at 90 seconds exposure time, (b) cell size distribution for the live (blue) and dead (red) cells after long-term (90 seconds) and short-term exposure time (30 seconds), (c) the fluorescence images of HeLa cells with pinhole disc in case of long and short-term exposure time.

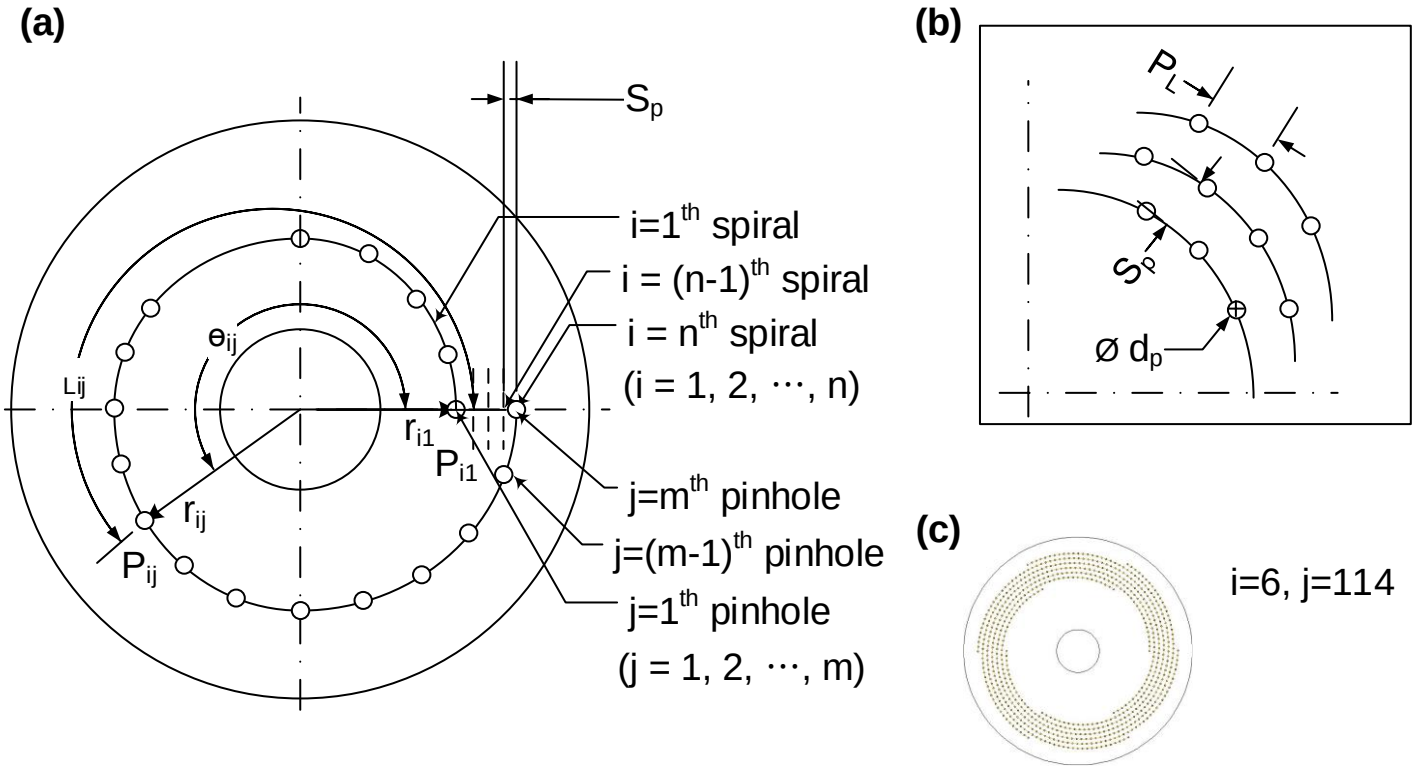

Figure 1. Design parameters for pinhole arrays and number of spirals to observe the whole specimen evenly by making the angular velocities of inner and outer pinholes same. (a) Related design parameters and nomenclatures for n number of spirals and m number of pinhole arrays, (b) Enlarged figure for the notation of pinhole specification and its position with a pitch of spirals, S_p, distance between each pinholes, P_L, and pinhole diameter, d_p, (c) An example of Autocad™ design of pinhole discs, which is following the parameter to design number of spiral is six and 114 pinholes array for each spiral.

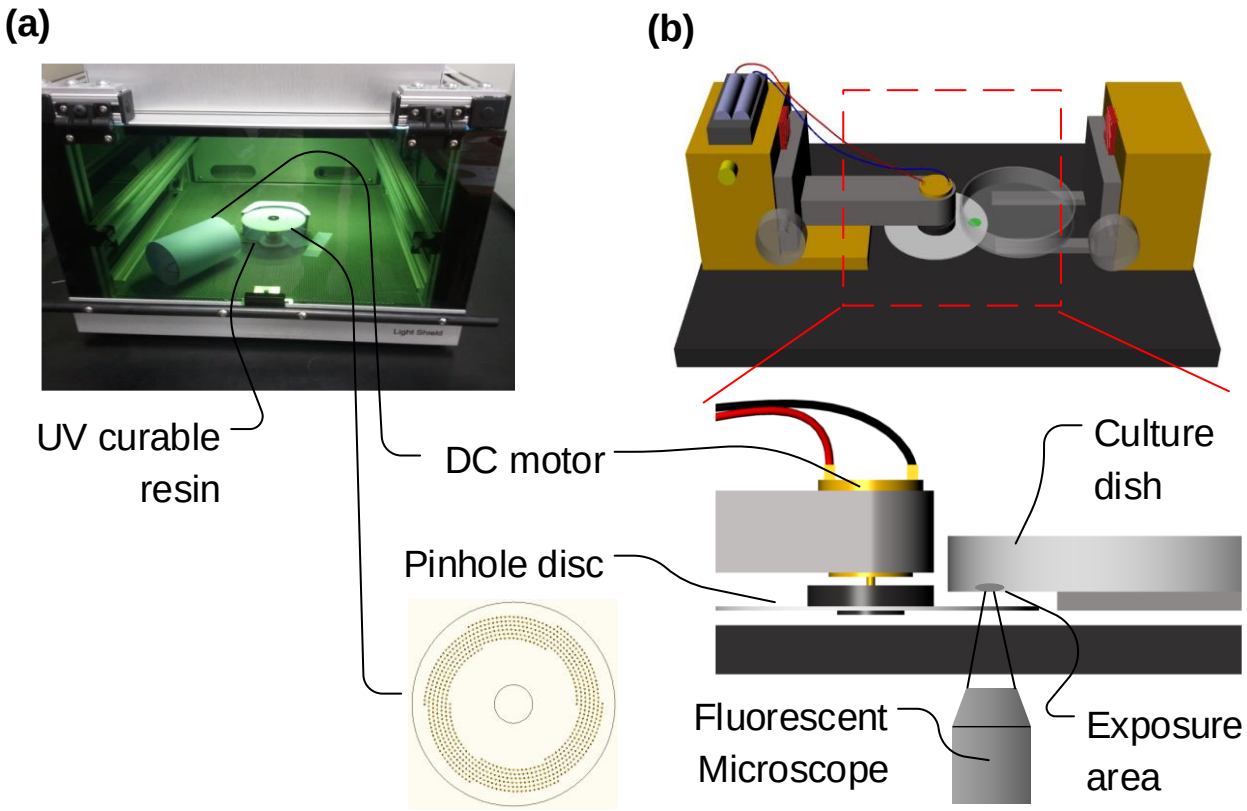

Figure 2. Schematic and photograph image of UV exposure test and cell imaging apparatus using a modified pinhole disc module. (a) UV curable resin exposure test apparatus using a rotated pinhole module which is set into the UV protective groove box, (b) Cultured cell imaging apparatus by using a conventional fluorescent microscope and a rotated pinhole disc module, which can be easily integrated into the conventional microscope system.

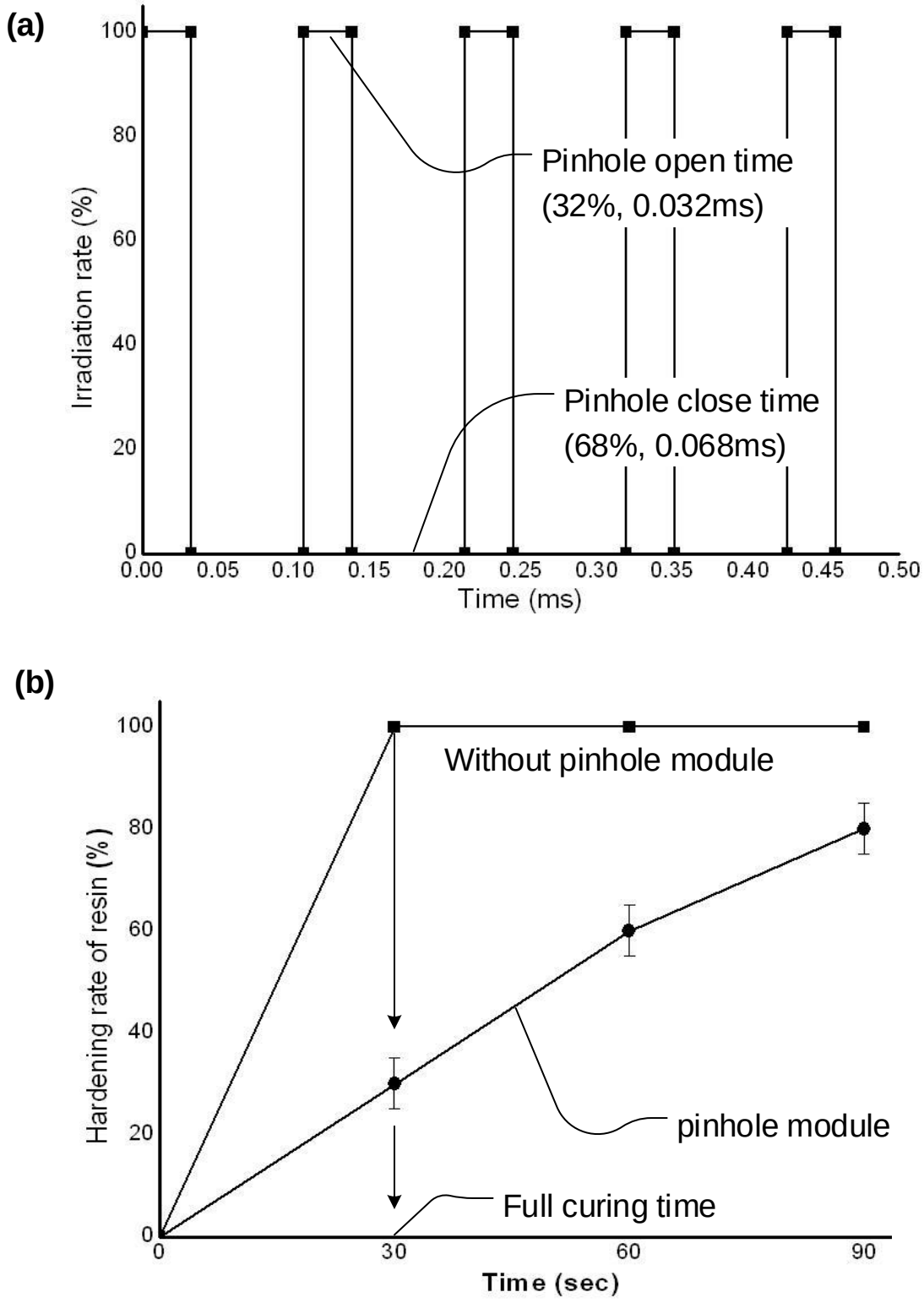

Figure 3. The results of the resin experiment in UV curing system by using pinhole disc module. (a) exposure rate (1:2.3) and average intensity of fluorescence (32%) onto a pinhole according to one disc rotation time with speed (523.6 rad/sec), (b) Hardening rate of the UV curable resin with and without using pinhole disc module according to exposure time until 90 second, each exposure time conditions were tested with three different samples to measure the hardening rate of resin. When 32% exposure duration is fixed with the pinhole geometry, the hardening rate of resin shows linear relationship with the exposure time in second time unit.

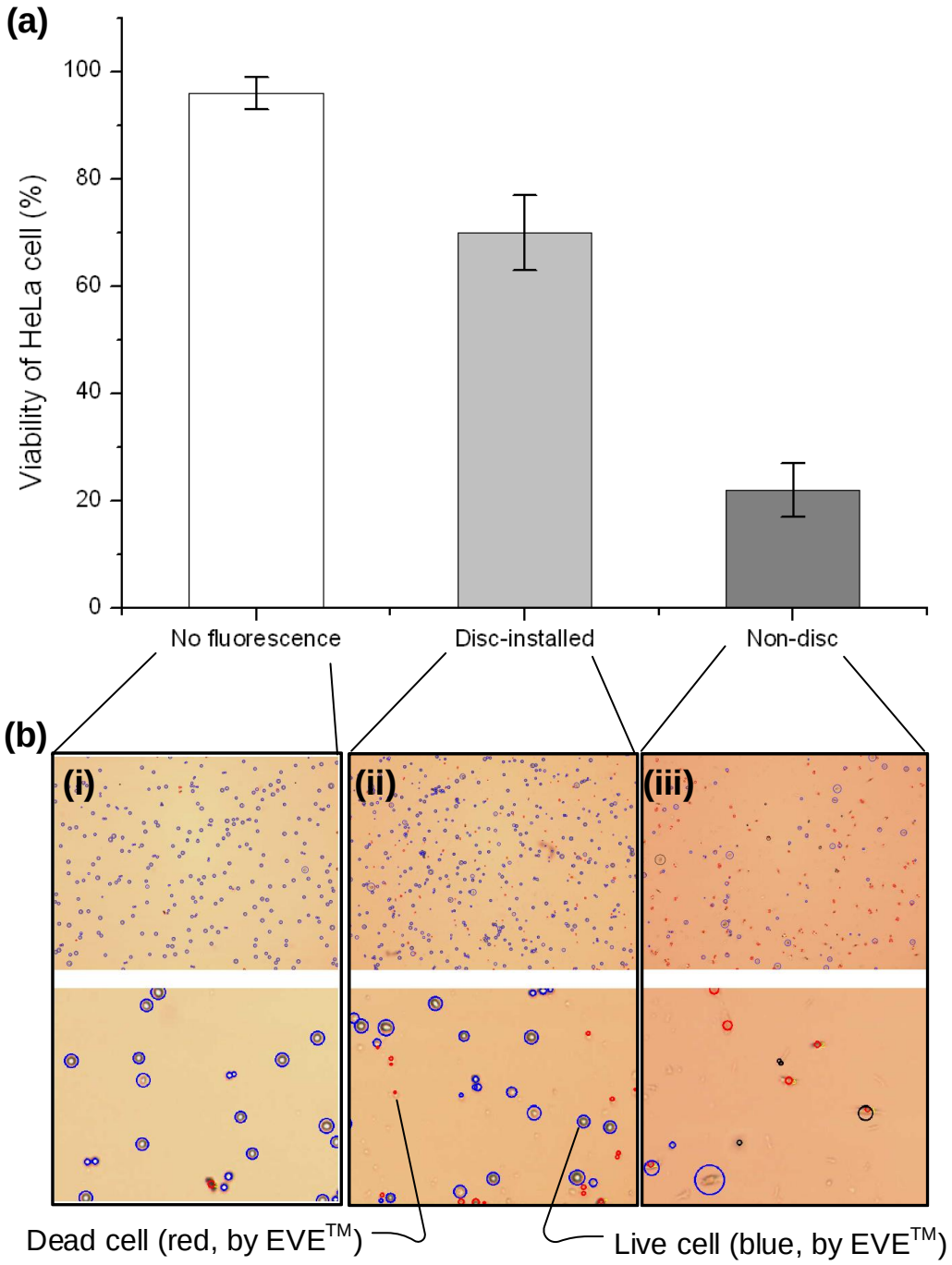

Figure 4. Cell viability test after pinhole disk exposure with cultured HeLa cells. (a) a graph of comparison of viability of cells with no fluorescence, exposure to fluorescence for 90 seconds with pinhole disc, and standard fluorescence imaging method without pinhole disc, (b)Trypan blue-stained HeLa cells' live/dead images measured with the EVE instrument and software: (i) no exposure to fluorescence, (ii) fluorescence exposure and pinhole disc, (iii) fluorescence exposure without pinhole disc

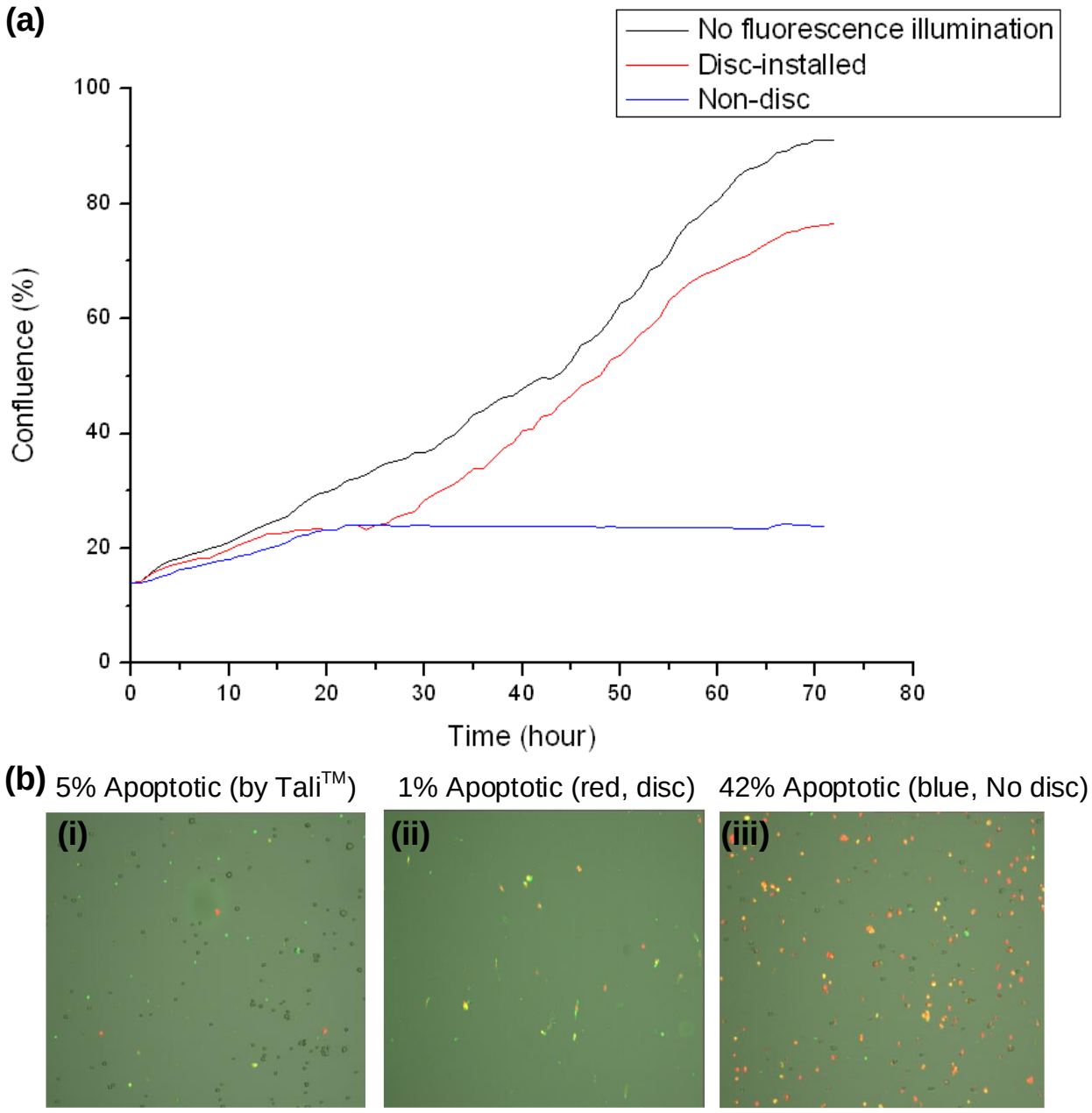

Figure 5. Confluence test after pinhole disk exposure with Live/Dead/Apoptotic cell death counting. (a) graph for the time vs confluence of the cultured cell, (b) A graph for confluence results of three types of HeLa cells cultured for 72 hours, (i) No exposure to fluorescence, (ii) Fluorescence exposure with pinhole disc, (iii) Fluorescence exposure without pinhole disc.

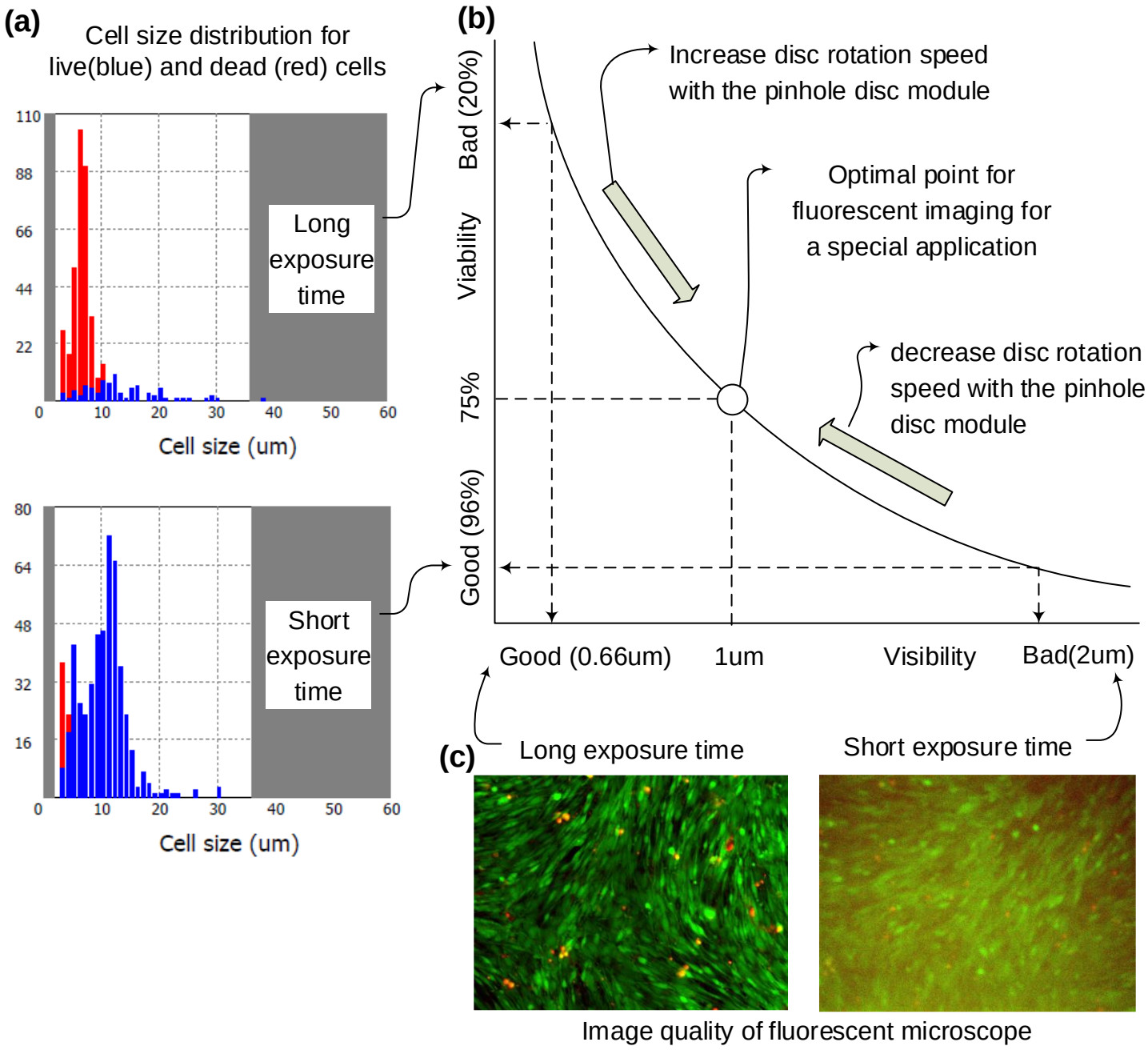

Figure 6. Schematic drawing for the optimal point of fluorescent imaging by adjusting disc rotation speed for viability and visibility compensation. (b) Optimal exposure time can be determined by changing the disc rotation speed. When the visibility increases, viability decreases. One example of the application can be to determine 1 um visibility with 75% viability at 90 seconds exposure time, (a) cell size distribution for the live (blue) and dead (red) cells after long-term (90 seconds) and short-term exposure time (30 seconds), (c) the fluorescence images of HeLa cells with pinhole disc in case of long and short-term exposure time.